ELSEVIER

Journal of Nuclear Materials 280 (2000) 120–125

journal of nuclear materials

www.elsevier.nl/locate/jnucmat

Letter to the Editors

Zr–silicide particles in Zr–2.5Nb pressure tube material: influence of oxidation and irradiation

Y.P. Lin *, V. Perovic

Ontario Power Technologies, 800 Kipling Ave., Toronto, Ont., Canada M8Z 6C4

Received 15 December 1999; accepted 9 March 2000

Abstract

Particles of Zr_3Si in a number of Zr–2.5Nb pressure tubes are found to exhibit segregation of Fe and Nb to the Zr_3Si/matrix interface. On oxidation between 583 and 673 K, an amorphous oxide of the silicide is formed. Neutron irradiation at 563 K resulted in no significant structural modifications to the silicide. The segregation of Fe and Nb to the silicide/matrix interface is retained after either oxidation or irradiation.

PACS: 28.41Qb; 61.16Bg; 61.72Ss; 82.80Ej

Zr–2.5 wt%Nb alloy is used as the material for pressure tubes in CANDU reactors. A significant difference between Zr–2.5Nb and other zirconium-based alloys, such as Zircaloys, used in the nuclear industry, is the nature of second phases and inclusion particles. Zr–2.5Nb contains both second phases and inclusion particles; the main second phases being β-Zr, β-Nb and the intermediate ω and Nb-enriched β-Zr phases related to the decomposition of the metastable β-Zr [1]. In Zircaloys, common second phase particles are $Zr(Fe, Cr)_2$ and $Zr_2(Fe, Ni)$ intermetallics in Zircaloy-2 and $Zr(Fe, Cr)_2$ in Zircaloy-4, although zirconium silicide particles are occasionally observed [2–6]. In Zr–2.5Nb, a variety of inclusion particles are also present; for example, $(Zr, Nb)_3Fe$ intermetallics have been reported [7] as was the presence of inclusions containing C, P and S [8,9]. Of more pertinence to the present work is the presence of silicide particles. Zirconium silicide particles in Zr–2.5Nb have been identified based on elemental analysis [8–10] or combined with electron diffraction analysis [11,12] and appear to be the most dominant inclusion in the alloy. A variation in the amount of zirconium silicide inclusions has been observed amongst different Zr–2.5Nb pressure tubes and the variation was suggested to be related to the different levels of deuterium pickup under reactor operating conditions [12] – the deuterium pickup being a phenomenon associated with the corrosion reaction between the pressure tube and the coolant at typically between 520 and 570 K. There is thus an interest in understanding the structural and microchemical changes that take place in the zirconium silicide particles due to corrosion/oxidation or irradiation. While the influence of oxidation [13,14] or irradiation [15] of intermetallic precipitates such as $Zr(Fe, Cr)_2$ [13–16] or $(Zr, Nb)_3Fe$ [15] has either been reported, little is known about the effect on zirconium silicide due to either oxidation or irradiation. The work described here addresses the effects of oxidation and of neutron irradiation on the nature of zirconium silicide particles and on the segregation of Fe and Nb to the particle/matrix interface.

Various Zr–2.5Nb pressure tube materials (2.5% Nb, 900–1300 ppm O, <1200 ppm Fe, <120 ppm Si, all by weight) used in the present work were manufactured by extrusion near 1100 K followed by cold drawing. Following tube manufacturing, the materials were heat treated for either 24 h at 673 K or 6 h at 773 K. For the oxidation investigation, one pressure tube material (H365M, heat treated for 6 h at 773 K) was subjected to

* Corresponding author. Tel.: +1-416 207 5986; fax: +1-416 236 0979.

E-mail address: yangpi.lin@oht.rd.hydro.on.ca (Y.P. Lin).

0022-3115/00/$ - see front matter
PII: S0022-3115(00)00047-7

oxide-forming exposures consisting of 24 h in 673 K steam followed by a total of 176 days in pH 10.5 lithiated water at 583 K. The overall oxide thickness determined using Fourier transform infra red spectroscopy was 2.2 μm. For the effect due to irradiation, a section of an ex-service pressure tube (P3L05, heat-treated for 24 h at 673 K prior to entering service) exposed to a fluence of 2.84×10^{25} nm^{-2} at 563 K was examined. An unirradiated section of P3L05 leftover from the initial installation was also examined.

For examination in the transmission electron microscope (TEM), plan-view oxide foils were prepared from mechanically thinned 3 mm disc. The metal at the central portion of the disc was dished using electropolishing at 233 K with a 10% perchloric acid/90% methanol electrolyte. Final thinning to electron transparency was achieved using an ion-mill operated with Ar^+ ions between 4 and 6 kV. Foils of the bulk alloy were prepared by electropolishing using a 10% perchloric acid/90% methanol electrolyte at 233 K. A JEOL 2010 TEM (200 kV) equipped with a LaB_6 filament was used for the examination of the thin foils. Oxide foils were additionally examined in a JEOL 2010F TEM (200 kV) equipped with a Field Emission Gun (FEG) source. Each of the microscopes was equipped with an Oxford instrument energy dispersive X-ray (EDX) spectroscopy system. The EDX detectors are of the ultra-thin window type and are capable of detecting light elements. A nominal 7 nm probe was used for analysis in the 2010 (LaB_6) microscope, while a nominal probe size of 0.7 nm was used in the 2010F (FEG) microscope.

Silicide particles were observed in a number of different Zr–2.5Nb pressure tube materials. Analysis of electron diffraction patterns showed that the crystal structure of the silicide particles was consistent with Zr_3Si [17]. Fig. 1 shows an example of a Zr_3Si particle in unoxidised, unirradiated pressure tube P3L05, a material known to contain a higher than usual density of often large silicide particles [12]. The associated (a) Si–K and Zr–L, (b) Fe–K and (c) Zr–K and Nb–K portions of EDX spectra, acquired using a nominally 7 nm probe, are shown in Fig. 2. Virtually identical results were obtained from silicide particles in the reference, unoxidised

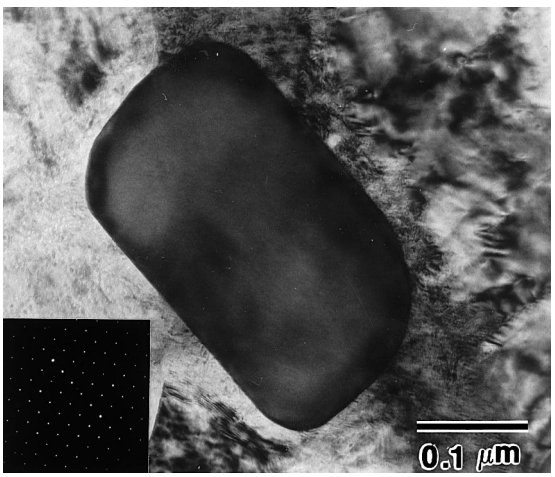

Fig. 1. Zirconium silicide particle in Zr–2.5Nb pressure tube P3L05. Inset shows [0 0 1] zone diffraction pattern from the silicide particle.

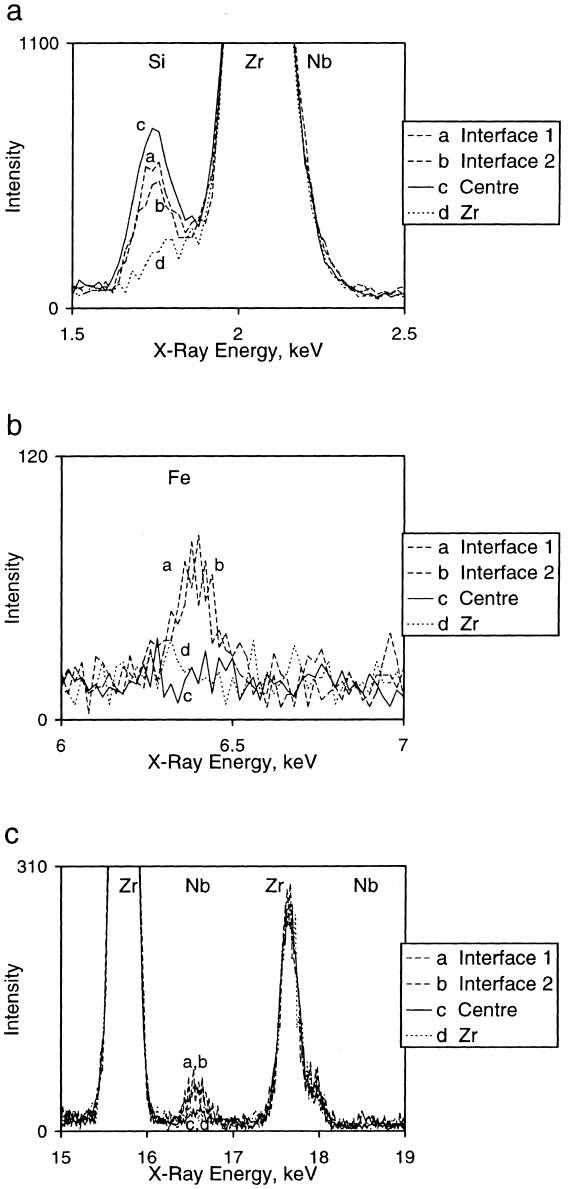

Fig. 2. (a) Si–K/Zr–L portion; (b) Fe–K portion; (c) Zr–K/Nb–K portion of EDX results from unoxidised silicide/α-Zr interface in pressure tube P3L05. All spectra have been scaled to the same (Zr–Kα + Nb–Kα) peak intensity.

H365M pressure tube and in a material that had received no cold-work and heat-treated for 1250 h at 583 K, i.e. at a lower temperature than the P3L05 and H365M materials. Present EDX results show that Fe was clearly present at the silicide/metal interface, while the level of Fe was below the detection limit in the α-Zr and at the centre of the silicide, Fig. 2(b). Similarly, Nb was concentrated at the interface, even though a small but above background amount of Nb was present throughout the silicide and in α-Zr, Fig. 2(c). A similar segregation of Fe and Nb around silicide particles in another Zr–2.5Nb alloy was reported by Griffiths et al. [10].

The observation of Fe and Nb segregation to the silicide/matrix interface in a number of pressure tubes further supports earlier observations that interfacial segregation is a common characteristic of Zr–2.5Nb pressure tube material [18]. The segregation does not appear to be influenced by different number densities and sizes of the silicide particles. The absence of sensitivity to post-extrusion heat treatments indicates that the segregation of Fe and Nb is a phenomenon established prior to or during the extrusion stage of pressure tube production.

Fig. 3 shows an oxidised silicide particles in an oxide foil. An enlarged portion of the particle is shown in Fig. 4(a). The main structural characteristic of the particle is the speckled image contrast. The speckled contrast did not vary with tilting of the foil in the TEM and is typical of amorphous materials. The amorphous nature of the oxidised silicide particle was confirmed by diffuse rings in the microdiffraction pattern shown as insert in Fig. 3. The amorphisation of silicide particles resembles the oxidation behaviour of β-Nb. Oxidised under similar conditions, β-Nb ultimately formed an amorphous oxide [19], on account of a low Nb mobility, relative to that of O, at the oxidation temperature [20]. In the case of zirconium silicide, a similar mobility/temperature consideration may account for the formation of an amorphous oxide structure, which may be additionally favoured by the covalent nature of the SiO_2 bonds.

The EDX analyses of various locations on and around the oxidised particle were conducted using a nominal 0.7 nm probe. The locations of analyses are marked in Fig. 4(b) and the results are shown in Fig. 5. Fig. 5(a) shows the presence of Si in the oxidised particle but not in the adjacent ZrO_2. Fig. 5(b) shows that Fe was depleted in the centre of the particle and in ZrO_2. The highest amount of Fe detected was at the interface between the oxidised silicide and ZrO_2. At locations mid-way between the particle centre and the interface,

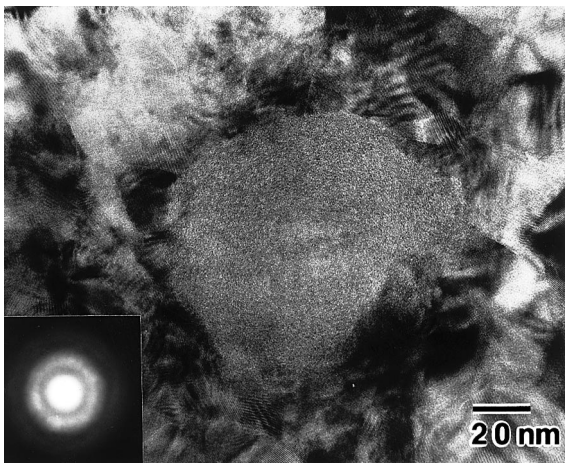

Fig. 3. Oxidised zirconium silicide particle showing speckled contrast typical of amorphous material. Inset shows microdiffraction pattern confirming amorphous nature of the oxidised silicide particle.

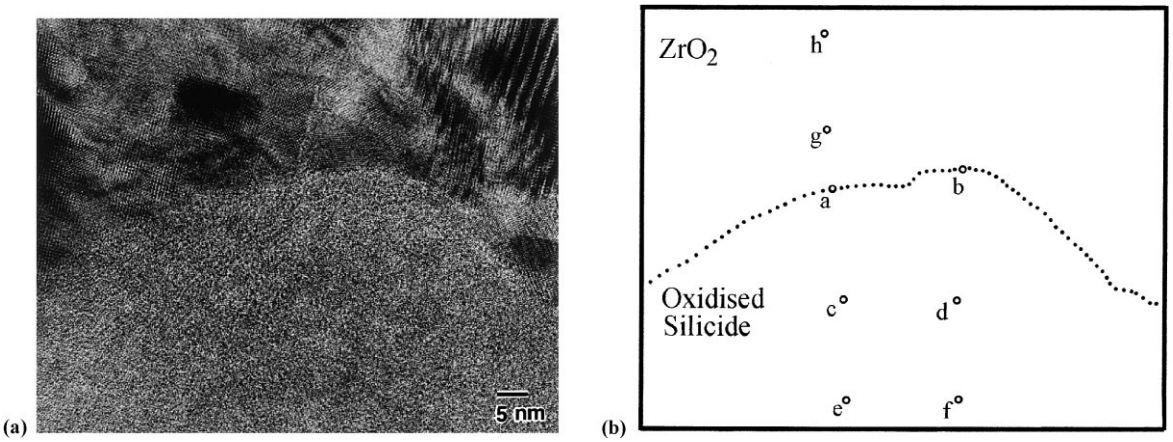

Fig. 4. (a) Portion of oxidised silicide particle shown in Fig. 3; (b) schematic diagram showing locations of EDX analyses.

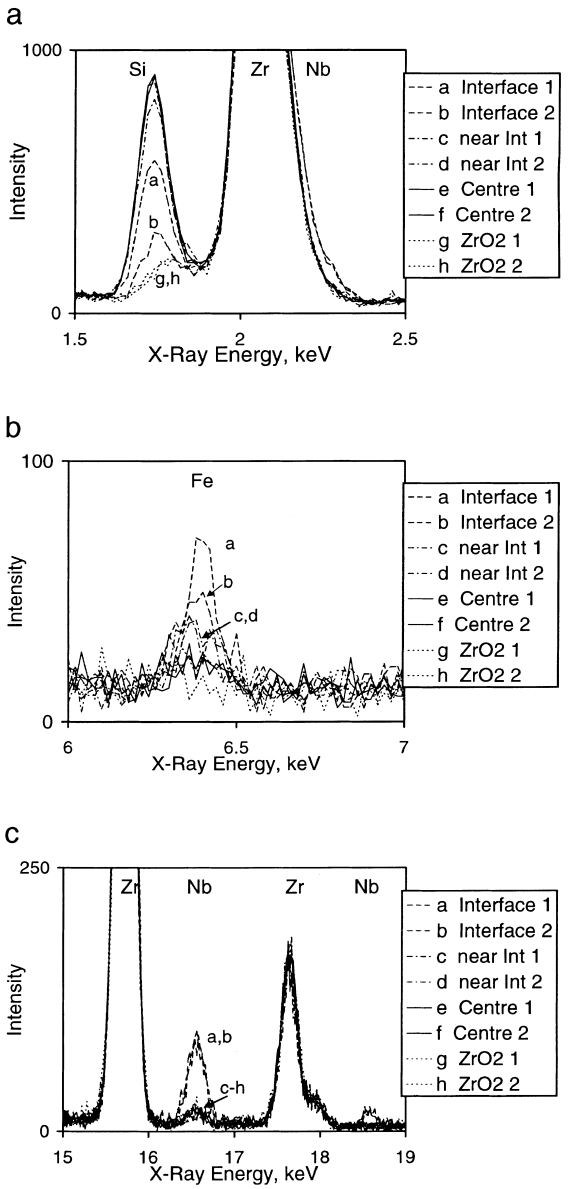

Fig. 5. (a) Si–K/Zr–L portion; (b) Fe–K portion; (c) Zr–K/Nb–K portion of EDX results from oxidised silicide/ZrO_2 interface. See Fig. 4(b) for locations of analysis. All spectra have been scaled to the same (Zr–Kα + Nb–Kα) peak intensity.

minor but detectable amounts of Fe were present. Minor amounts of Nb were generally present throughout the oxidised precipitate and ZrO_2; however Nb was substantially concentrated at the particle/ZrO_2 interface as shown in Fig. 5(c). (The interfacial Nb segregation is also evident in the Nb–L portion of spectra, Fig. 5(a).)

The Nb/Zr ratio at the oxidised silicide/ZrO_2 interface, Fig. 5(c), superficially appears different than at the unoxidised interface, Fig. 2(c). However, the extent of segregation before (Fig. 2(c)) and after (Fig. 5(c)) oxidation cannot be directly compared, due to the different probe sizes available in the different microscopes. Nevertheless, present results show that the interfacial segregation of Fe and Nb associated with silicide particles did not diminish as a result of oxidation. Such a retention of elemental distribution after oxidation is consistent with the correspondence between the microstructures of Zr–2.5Nb alloy and its oxide, especially with respect to the segregation of Nb and Fe in β-Zr regions [19].

The high spatial resolution EDX results in Fig. 5(b) show that some Fe appear to be present in regions adjacent to the oxidised silicide interface. A similar Fe distribution in the unoxidised silicide is expected to be present which would not be observable in the EDX results obtained using a coarse electron probe as shown in Fig. 2.

A zirconium silicide particle from the irradiated pressure tube P3L05 is shown in Fig. 6. The presence of lattice fringes throughout the silicide shows that the crystallinity of the silicide was not affected by neutron irradiation. Analysis of electron diffraction patterns confirmed a Zr_3Si crystal structure with lattice parameters indistinguishable from those of Zr_3Si in unirradiated pressure tubes. The associated comparison of EDX spectra obtained from the centre and edge of the particle is shown in Fig. 7. The main findings are essentially similar to those from unirradiated silicide, Fig. 2, i.e. Fe and Nb are both segregated to the silicide/matrix interface. In the case of Nb, an appreciable background level was present due to the irradiated nature of the sample. Despite this interference, the presence of Nb segregation to the interface is evident in Fig. 7(c).

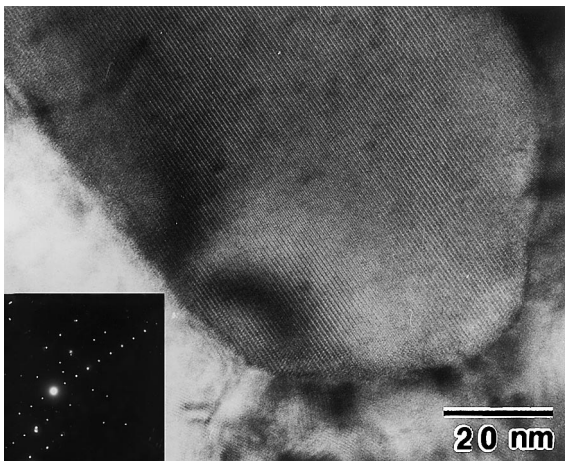

Fig. 6. Zirconium silicide particle showing lattice fringes in irradiated pressure tube P3L05 (fluence 2.84×10^{25} nm^{-2} at 563 K). Inset shows associated diffraction pattern.

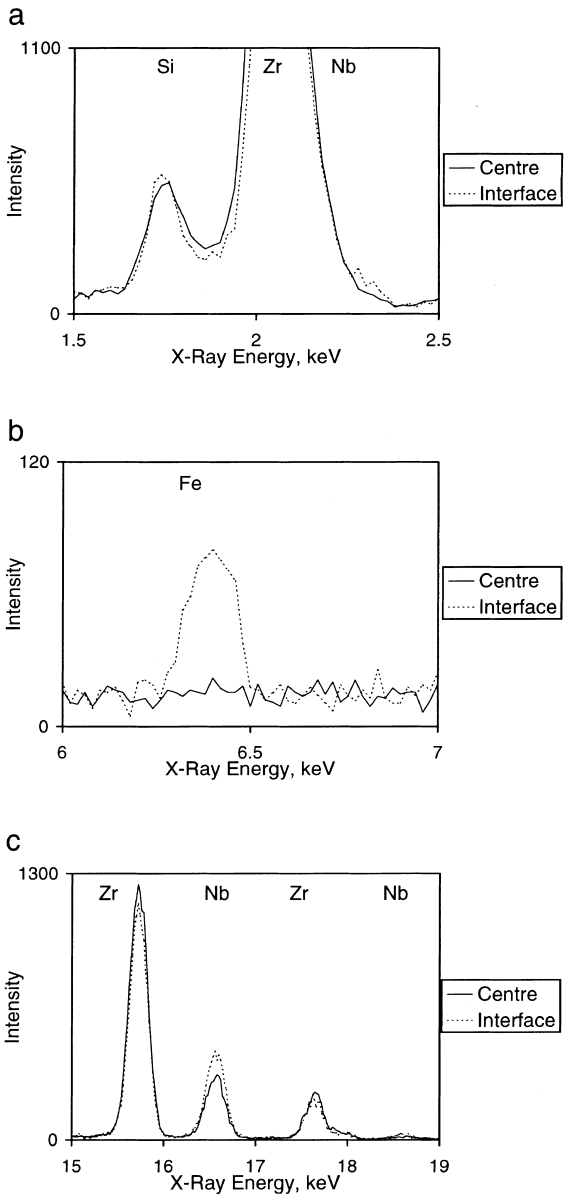

Fig. 7. (a) Si–K/Zr–L portion; (b) Fe–K portion; (c) Zr–K/Nb–K portion of EDX results from irradiated but unoxidised silicide particle in pressure tube P3L05. All spectra have been scaled to the same (Zr–Kα + Nb–Kα) peak intensity.

Under present irradiation and corrosion conditions, neither oxidation nor irradiation affected the segregation of Fe and Nb, suggesting that the silicide/matrix interface persisted as a strong sink for these elements. The association of Fe with Nb is consistent with results of near-edge structure investigations showing segregated Fe in Zr–2.5Nb alloys existed in a form more akin to ZrNbFe than pure metallic iron or known compounds with zirconium [21].

In summary, segregation of Fe and Nb to the silicide/matrix interface in Zr–2.5Nb pressure tube materials is observed. The segregation is not sensitive to the thermomechanical history of the pressure tube and is not influenced by the inclusion density. The silicide particles become amorphous when oxidised at between 583 and 673 K. Neutron irradiation at 563 K up to 2.84×10^{25} nm^{-2} did not cause significant structural changes. The presence of Fe and Nb segregation to the silicide/matrix interface is qualitatively unaffected either by irradiation or by oxidation.

Acknowledgements

The authors would like to thank J. DeLuca and R. Jarochowicz of Ontario Power Technologies for technical assistance and Dr O. T. Woo of AECL Chalk River Laboratories for useful discussions. This work was funded by Ontario Power Technologies and CANDU Owner's Group.

References

[1] B.A. Cheadle, S. Aldridge, J. Nucl. Mater. 47 (1973) 255.
[2] T. Andersson, T. Thorvaldsson, A. Wilson, A.M. Wardle, IAEA-SM-288/59, in: Proceedings of International Symposium on Improvements in Water Reactor Fuel Technology and Utilization, Stockholm, 15–19 September 1986, IAEA, Vienna, 1987, p. 435.
[3] G. Maussner, E. Steiberger, E. Tenckhoff, ASTM STP 939, in: Proceedings of Seventh International Symposium on Zirconium in the Nuclear Industry, Strassbourg, France, 24–27 June 1985, ASTM, Philadelphia, 1987, p. 307.
[4] N.V. Bangaru, R.A. Busch, J.H. Schemel, ASTM STP 939, in: Proceedings. of Seventh International Symposium on Zirconium in the Nuclear Industry, Strassbourg, France, 24–27 June, 1985, ASTM, Philadelphia, 1987, p. 341.
[5] P. Rudling, M.M. Lindback, B. Lethinen, H-O. Andren, K. Stiller, ASTM STP 1245, in: Proceedings of 10th International Symposium on Zirconium in the Nuclear Industry, Baltimore, MD, USA, 21–24 June, 1993, ASTM, Philadelphia, 1994 p. 599.
[6] D. Cherquet, E. Alheritiere, ASTM STP 939, in: Proceedings of Seventh International Symposium on Zirconium in the Nuclear Industry, Strassbourg, France, 24–27 June, 1985, ASTM, Philadelphia, 1987, p. 284.
[7] O.T. Woo, G.J.C. Carpenter, in: Proceedings of 12th Inter. Cong. on Electron Microscopy, San Francisco Press, 1990, p. 132.
[8] P.H. Davies, I. Aitchison, D.D. Himbeault, A.K. Jarvine, J.F. Watters, Fatigue Fract. Eng. Mater. Structures 18 (1995) 789.
[9] A.J. Lockley, Microstruct. Sci. 22 (1994) 39.
[10] M. Griffiths, W. Phythian, S. Dumbill, J. Nucl. Mater. 207 (1993) 353.
[11] O.T. Woo, private communication.

[12] N. Ramasubramanian, V. Perovic, M. Leger, in: Proceedings of 12th International Symposium on Zirconium in the Nuclear Industry, Toronto, Canada, June 1998 (ASTM, Philadelphia), to be published as ASTM STP, p. 1354.
[13] D. Pecheur, F. Lefebvre, A.T. Motta, C. Lemaignan, J. Nucl. Mater. 189 (1992) 318.
[14] D. Pecheur, F. Lefebvre, A.T. Motta, C. Lemaignan, D. Charquet, ASTM STP 1245, in: Proceedings of 10th International Symposium on Zirconium in the Nuclear Industry, Baltimore, USA, 21–24 June, 1993, ASTM, Philadelphia, 1994, p. 687.
[15] M. Griffiths, J.F. Mecke, J.E. Winegar, ASTM STP 1295, in: Proceedings of 11th International Symposium on Zirconium in the Nuclear Industry, Garmisch-Partenkirchen, Germany, 11–14 September, 1995, ASTM, Philadelphia, 1996, p. 580.
[16] M. Griffiths, R.W. Gilbert, G.J.C. Carpenter, J. Nucl. Mater. 150 (1987) 53.
[17] H. Okamoto, in: Binary Alloy Phase Diagrams, American Society for Metals, Metals Park, 1990, p. 3382.
[18] V. Perovic, A. Perovic, G.C. Weatherley, G.R. Purdy, J. Nucl. Mater. 224 (1995) 93.
[19] Y.P. Lin, O.T. Woo, J. Nucl. Mater. 277 (1999) 11.
[20] O. Thomas, F.M.D. Heurle, A. Charai, Philos. Mag. B 58 (1988) 529.
[21] L.M. Brown, C.A. Walsh, A. Dray, A.L. Bleloch, Microsc. Microanal. Microstruct. 6 (1995) 121.